Journal of Colloid and Interface Science 356 (2011) 526–535

Contents lists available at ScienceDirect

Journal of Colloid and Interface Science

www.elsevier.com/locate/jcis

Multifunctional NO-delivery vessel derived from aminopropyl-modified mesoporous zeolites

Feng Wei, Qian Hou, Jia Yuan Yang, Jian Hua Zhu *

Key Laboratory of Mesoscopic Chemistry of MOE, School of Chemistry and Chemical Engineering, Nanjing University, Nanjing 210093, China

ARTICLE INFO

Article history:
Received 12 November 2010
Accepted 5 January 2011
Available online 11 January 2011

Keywords:
NO delivery
Mesoporous zeolite
Aminopropyl functionization
Adsorption of nitrosamines
Bifunctional material

ABSTRACT

A new strategy, releasing nitric oxide (NO) and adsorbing nitrosamines simultaneously by zeolitic materials in the digestive system, is validated in this paper. Three types of moisture-saturated molecular sieves, HZSM-5 zeolite, mesoporous zeolite, and mesoporous silica MCM-41, are used as NO-delivery vessels in mimic gastric juice after modification of γ-aminopropyltriethoxysilane (APTES). APTES modification dramatically increased the capability of zeolite and mesoporous silica in NO release in acidic solution, because more NO can be adsorbed in the composite and stored in the form of nitrite. Some composites released the NO 10 times more than their parent materials, and synchronously captured the carcinogen nitrosamines in mimic gastric juice. The influences of APTES modification on the porous structure and surface state of zeolite and mesoporous silica were investigated by XRD, N_2 adsorption, and FTIR tests, through which the mesoporous zeolite is proven to be the optimal support. With this hierarchical material a controllable APTES modification is realized in which a lot of aminopropyl groups are grafted in mesopores while the zeolitic structure is maintained, so the resulting sample exhibits a high capability in releasing NO and adsorbing nitrosamines. This investigation provides a clue for elevating the efficiency of zeolites in the application of life science.

1. Introduction

Drug-delivery systems (DDS), acting as vehicles to deliver drugs into a biological system [1,2], are important for health care and biotechnology; therefore, various types of DDSs are continually developed to improve chemotherapy efficacy and reduce their adverse effects [2–5]; among them zeolite is an attractive candidate. However, DDS is not only a potential application of zeolite and other molecular sieves in life science but also lodges challenge for these selective adsorbents. For instance, two challenges arise from the NO-delivery process: First, the manner of introduction of the drug-delivery material would affect its actual performance in an organism. Can zeolitic materials bring a better NO-release route? Second, there are many reports on the controlled release of a guest from drug-embedded composites at the target site [5,6], but most of these matrices only play the role of support. Can these selective adsorbents exert the adsorption and/or catalysis function simultaneously in the delivery process? From the point of view that hemoglobin transports oxygen and takes carbon dioxide in the blood vessel, we plan to develop a novel multifunctional zeolitic vessel as both an efficient releaser and a selective trapper.

NO is essential for life at very low concentrations [7,8]. It can be diffused readily across cell membranes [9], mediating a number of vital functions in the cardiovascular, nervous, and immune systems, such as vasodilatation [10,11], blood pressure regulation and vascular smooth muscle cell relaxation [12,13], inhibition of platelet aggregation [5], and so on. Delivery of exogenous NO is attractive for overcoming some diseases resulting from NO insufficiency [14–16]. In particular, quantum dots, metallic and silica nanoparticles, and metal organic frameworks (MOFs) are used as NO-delivery materials [17]. However, in some cases the materials need to directly contact blood, which could induce potential dangers with the formation of blood clots because the particles are at the nanometer level in the blood vessel [18]. Moreover, those transition metal cations utilized to elevate the release ability of the compound would be potentially harmful in practical applications for human [19]. Fabricating an NO-releasing sock or bandage is another strategy for delivery of NO to the wound or target sites [20]. Unfortunately, in the acidic milieu of human skin, the easily formed acidified nitrite has been found to induce an intense cutaneous inflammatory infiltrate [21]. Medicines such as sodium nitroprusside, nitroglycerin, amyl nitrite, and nicorandil are commonly used as cardiovascular drugs to modulate the bioactivity of NO; however, NO-delivery materials entering into the digestive system seem to have less danger than those entering the circulatory system. Actually, NO as an active species for antiulcer action in the stomach has already been proposed, and it can also initiate mucus secretion and cell proliferation during the ulcer-healing process to promote lesion repair [22,23]. Unlike the delivery of

* Corresponding author. Fax: +86 25 83317761.
E-mail address: jhzhu@netra.nju.edu.cn (J.H. Zhu).

0021-9797/$ - see front matter © 2011 Elsevier Inc. All rights reserved.
doi:10.1016/j.jcis.2011.01.019

NO in the circulatory system where the carrier starts to release once in contact with moisture, acid-triggered release is characteristic of NO delivery in the digestive system [24], in which the delivery materials are immerged in gastric juice. Thus it is challenge for them to maintain the high efficiency of release and more difficult, to selectively eliminate the carcinogen nitrosamines at the same time.

Nitrosamines induce tumor and cancer even in trace amounts in almost all organs of experimental animals [25,26], but they require metabolic activation before reaction with DNA to cause mutation and cancer. Thus, preventing the carcinogens from metabolic activation is necessary in the struggle against cancer so that removal of nitrosamines in gastric juice is important for health care. To perform the transportation of NO and the adsorption of nitrosamines into the stomach, the choice and fabrication of vessel materials are vital. The low toxicity, controlled selective adsorption ability, and biocompatibility of zeolites are suitable for NO-delivery materials in a biological system [27,28]. Acidic zeolite can also degrade nitrosamine at ambient temperature to form NO product [29], not only eliminating the carcinogenicity of nitrosamines but also *in situ* generating NO. Nonetheless, adsorption of nitrosamines by zeolite in aqueous solution is not easy because of the interference of water so that the hydrophobic zeolite should be utilized. Consequently zeolite HZSM-5 is selected because of its adsorption performance in acid solution [25]. Three other types of mesoporous samples, the mesoporous zeolite containing ZSM-5 structure, the Al-containing, and the siliceous MCM-41 mesoporous materials, are also chosen to explore the influence of mesopore and Al component on their performance.

Organic modification of vessel materials is important for elevating their NO-delivery efficiency [30]. In particular, amine can react with NO to promote adsorption of NO and the release in acidic solution [31], but its drawbacks of forming nitrosamines and leaching amino groups hinder its application [30]. Thus, γ-aminopropyltriethoxysilane (APTES) is selected to be the modifier because it can improve the adsorption of nitrosamines in tobacco-extracted solution [32], which is valuable for "releasing while adsorbing" multifunctional biomaterials. However, suspicion still exists on multifunctional materials in mimic gastric juice. Once the porous material releases the preadsorbed NO, would it affect the following trapping of nitrosamines in the acidic solution? Would the modified organic groups catalyze the released NO to form nitrosamines in the solution? To answer these questions would not only provide a novel multifunctional biochemical vessel but also elevate the efficiency of molecular sieves in their potential application in health care. Two types of nitrosamines, *N*-nitrosopyrrolidine (NPYR), the volatile monocyclic nitrosamine with a five-member ring, and *N*-nitrosonornicotine (NNN), one of bulky tobacco-specific nitrosamines, are used as the targets and put into the mimic gastric juice to assess the selective adsorption ability of the organic-modified zeolite and molecular sieves.

2. Experimental

2.1. Materials

HZSM-5 zeolite with a Si/Al ratio of 20 was obtained by ion exchange from parent zeolite NaZSM-5 [33]. NPYR and NNN were purchased from Sigma and Toronto Research Chemicals, respectively. Silica aerogel was obtained from Qingdao Haiyang (China), cetyltrimethylammonium bromide (CTAB), and APTES were the products of Shanghai Lingfeng and Nanjing Xiangfei (China), respectively. Hydrochloric acid and sodium hydroxide were procured from Nanjing Chemical Reagent, and other reagents with AR grade were used as received without further purification.

2.2. Preparation

Mesoporous silica MCM-41 and its Al-containing analogue with a Si/Al ratio of 33 were synthesized according to the literature [34], and the resulting samples were denoted as MS and M33, respectively. Mesoporous zeolite was prepared by a dry-gel conversion method [35]: One gram of as-synthesized mesoporous material M33 was added into TPAOH ethanol solution (0.5 g 25% TPAOH solution mixed with 10 g ethanol), and then stirred for 0.5 h. Subsequently, the resulting mixture was evaporated at 353 K followed by heating at 453 K for 24 h. The obtained sample was then washed with water, air-dried, and finally calcined in air at 823 K for 5 h to give a product named as MZ, which represents mesoporous zeolite.

Aminopropyl-functionalized HZSM-5 zeolite, mesoporous zeolite, and MCM-41 mesoporous materials were carried out by post-modification as follows: 0.5 g calcined support was mixed with a 50 ml chloroform solution of APTES (0.1, 0.05, or 0.02 M) and stirred for 24 h at room temperature, and then the precipitate was filtered and washed with chloroform [36]. The obtained composites were named as *n*AZ, *n*AMS, *n*AM33, or *n*AMZ, where "*n*" and "A" represent the concentration of APTES used in initial solution and APTES, respectively, and "Z" means HZSM-5 zeolite. All samples were conditioned at ambient temperature at 79% relative humidity prior to use.

A half liter of fasting gastric juice with a pH value of 1.2 was prepared by adding 0.35 g NaCl, 0.5 g glycine, and 31.6 ml 1 M hydrochloric acid into distilled water, giving the blank mimic solution. For some experiments the quantitative NPYR or NNN was added into the mimic gastric juice [26]. The container was kept at 277 K to avoid the volatilization of NPYR or NNN.

2.3. Characterization

The X-ray diffraction (XRD) patterns of samples were recorded on an ARL XTRA diffractometer with Cu Kα radiation in the 2-theta range from 1° to 6° or from 5° to 50° [37]. The nitrogen adsorption and desorption isotherms were measured at 77 K on a Micromeritics ASAP 2020 volumetric adsorption analyzer, and about 100 mg of samples was evacuated at 573 K for 4 h in the degas port of the adsorption analyzer prior to tests. However, organosilane-functionalized samples were evacuated at 373 K for 5 h before measurement. The BET specific surface areas of composites were calculated using adsorption data in the relative pressure range from 0.04 to 0.2, while their total pore volume was determined from the amount adsorbed at a relative pressure of about 0.99. Their micropore areas and micropore volume were calculated by the *t*-plot method, according to statistical film thickness (t) in the range 0.35–0.50 nm. The pore size distribution curves of samples were evaluated from adsorption branches of the isotherms using the BJH method [32], and their Si/Al ratio was determined with a ARL-9800 X-ray fluorescence (XRF) spectrometer, while the N contents of these APTES-functionalized samples were measured by Heraeus CHN-O-Rapid element analyzer. Infrared tests were performed on a set of Bruker Vedtor22 combined with the conventional KBr wafer technique.

In situ FTIR spectra for NO adsorbed on samples were recorded on a Nicolet 5700 FTIR spectrometer. The sample disk with an area density of 20 mg cm^{-2} was purged with N_2 flow for 5 min at 310 K prior to taking a background spectrum, and then exposed to a stream of NO–N_2 (1.98% of NO by volume) flow at a rate of 5.0 ml min^{-1} for 0.5 h, followed by a purge with N_2 flow for 1 h. All spectra were taken at 310 K and subtracted with the corresponding background.

Adsorption of NO was performed at 310 K. Sixty milligrams of sample (20–40 mesh) filled the Pryrex glass reactor and the NO–N_2 mixture with 0.8 μmol of NO was injected every 1 min in the

N_2 flow with a rate of 30 ml min^{-1}. The number of injections was fixed to 30 [38], and then the sample was purged by the N_2 flow for 1 h.

The sample preadsorbed with NO (30 mg) was immediately added into 15 ml mimic gastric juice solution with pH 1.2. The experiment was carried out at 310 K for 2 h, and the desorbed amount of NO was detected every 30 min [20]. The NO_2 released from the zeolite was removed by NaOH and thus NO became predominant in the desorbed gases. Subsequently, the residual mixture was centrifuged at 3000 rpm for 15 min to separate the solution and solid. Then 10 ml of the clean solution was extracted by 60 ml dicholoromethane and concentrated to a final volume of 25 ml. The residual concentration of NPYR or NNN in the mimic gastric juice was determined by improved spectrophotometric methods [26].

3. Results

3.1. Characterization of APTES-modified composites

Table 1 lists the loading amount of APTES on various samples. The smallest amount of APTES was coated on HZSM-5 zeolite under the same conditions; for instance, only 0.75 and 1.07 wt.% of N were detected on 0.02AZ and 0.1AZ samples, less than that on 0.02AMZ (2.03%) and 0.1AMZ (4.08%), respectively, due to fewer silanol groups, smaller surface area, and narrow channel of the zeolite. Mesopores and large surface area of support were beneficial for modification with APTES; hence, the organic-modified composites had an increasing tendency of N level: 0.1AZ < 0.1AMZ < 0.1AM33. Also, the Al component seemed to promote the organic modification of mesoporous silica, because 0.1AMS had a lower N level than the 0.1AM33 sample (Table 1). Fig. 1A shows the low-angle XRD patterns of mesoporous samples before and after modification with APTES. MS and M33 samples showed three peaks that could be indexed to (1 0 0), (1 1 0), and (2 0 0) reflections of hexagonal structure, but their reflection intensity was lowered after APTES modification because aminopropyl groups were loaded inside mesopores, leading to low scatter contrasts between pore walls and pore space [39]. The MZ sample had a broadened peak in the pattern, implying the preservation of mesosphase along with disordered structure and enlarged unit cell [35]; APTES modification made its order of structures gradually decreased. On the contrary, APTES modification had an innocuous effect on the framework symmetry of HZSM-5 zeolite, and no obvious change was observed on the structure of *n*AZ (Fig. 1B). Likewise, *n*AMZ materials preserved all characteristic peaks of MFI zeolite despite the variation in the intensity of the main peaks (Fig. 1B).

Fig. 2A illustrates the nitrogen adsorption–desorption isotherms of MCM-41 and its Al-containing analogues. These composites had isotherms of type IV with a step increased at p/p_0 = 0.2–0.35, reflecting their narrow pore size distribution. Another hysteresis loop also appeared on the M33 sample at high pressure, originating from the capillary agglomeration in these relatively large mesopores [40]. Modification with APTES made both 0.1AMS and 0.1AM33 composites lose their characteristic of type IV isotherms and their surface areas and pore volumes were drastically reduced (Table 1 and Fig. 2B). It is noteworthy that a hysteresis loop was still observed at the high relative pressure, implying that APTES anchored on the wall surface and did not obviously block the large mesopores of the 0.1AM33 sample. Fig. 2C delineates the nitrogen adsorption–desorption isotherms of MZ and *n*AMZ samples. An obvious hysteresis loop emerged on the spectrum of mesoporous zeolite MZ at a high relative pressure, along with a rapid increase in nitrogen uptake at a relative pressure p/p_0 of 0–0.2, indicating the coexistence of micropores and mesopores. As is evident from Fig. 2D, the adsorbed volume of *n*AMZ samples was lowered as more APTES was introduced, and their primary pore size became indistinct in the mesopore region. Also, the BET surface area and total pore volume of *n*AMZ samples decreased whereas their micropore volume and micropore surface area increased because more aminopropyl groups anchored in their mesochannels to form new micropores (Table 1 and Scheme S1A). The hysteresis loop at a relative pressure p/p_0 of 0.4–1 was still observed, indicating the reserve of mesopores on *n*AMZ samples. Similarly, both the surface area and the pore volume of *n*AZ samples were also lowered as the content of aminopropyl in the composites increased (Table 1 and Fig. S1).

Fig. 3 shows FTIR spectra of MCM-41 series samples. The bands of 1080, 805, and 455 cm^{-1} that associated with condensed silica network were observed on MS and M33, but the 960 cm^{-1} band assigned to Si–OH bending vibration was weaker on M33, because incorporation of aluminum in the composite reduced the

Table 1
Structural parameters of porous materials and adsorption of nitrosamine in mimic gastric juice by samples preadsorbed with NO at 310 K.

Sample	HZSM-5	0.02AZ	0.1AZ	MZ	0.02AMZ	0.05AMZ	0.1AMZ	M33	0.1AM33	MS	0.1AMS
Si/Al	20.0	21.2	21.5	29.0	32.8	33.5	40.4	33.4	51.1	0	0
Pore size (nm)	0.54 × 0.56	/	/	3.45	2.33	/	/	2.50	/	2.48	/
S_{BET} ($m^2\ g^{-1}$)	319	127	89	593	336	278	264	1097	164	1119	366
S_{mic} ($m^2\ g^{-1}$)	209	107	65	121	94	112	117	0	73	0	218
V_{total} ($cm^3\ g^{-1}$)	0.17	0.07	0.05	0.62	0.32	0.26	0.27	1.11	0.20	0.94	0.23
V_{mic} ($cm^3\ g^{-1}$)	0.10	0.05	0.03	0.05	0.04	0.05	0.05	0	0.03	0	0.10
N (%)	0	0.75	1.07	0	2.03	2.29	4.08	0	5.40	0	4.30
Aminopropyl (mmol g^{-1}) (A)	/	0.54	0.76	/	1.45	1.64	2.91	/	3.86	/	3.07
Loading efficiency (%)[a]	/	27	7.6	/	72.5	32.8	29.1	/	38.6	/	30.7
NPYR											
Q_e (mg g^{-1})[b]	0.71	0.63	0.49	0.58	0.19	0.22	0.33	0.10	0	0.02	0
Q_s (μg m^{-2})[c]	2.23	4.96	5.51	0.98	0.57	0.79	1.25	0.09	0	0.02	0
Removed (%)[d]	82.6	73.3	57.0	67.4	22.1	25.6	38.4	11.6	0	2.3	0
NNN											
Q_e (mg g^{-1})[b]	0.26	0.27	0.28	0.33	0.18	0.21	0.27	0.33	0.13	0.30	0.16
Q_s (μg m^{-2})[c]	0.82	2.13	3.15	0.56	0.54	0.76	1.02	0.30	0.79	0.27	0.44
Removed (%)[d]	50.5	52.4	54.4	64.1	35.0	40.8	52.4	64.1	25.2	58.3	31.1

[a] A divided relevant APTES content in the initial solution. (0.02, 0.05, or 0.1 M APTES in the system corresponding to 2, 5, or 10 mmol g^{-1} of APTES on the sample, respectively).
[b] The concentrations of NPYR and NNN in mimic stomach juice were 1.72 and 1.03 mg L^{-1}, respectively.
[c] Adsorption amount per square meter.
[d] Removal efficiency of nitrosamine.

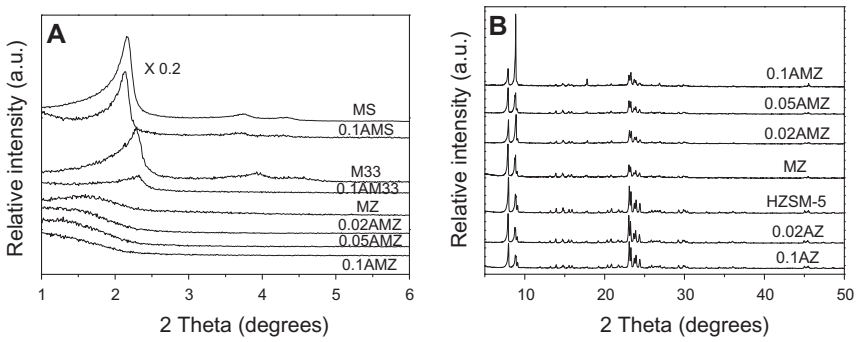

Fig. 1. (A) Low-angle and (B) wide-angle XRD patterns of molecular sieves before and after modification with APTES.

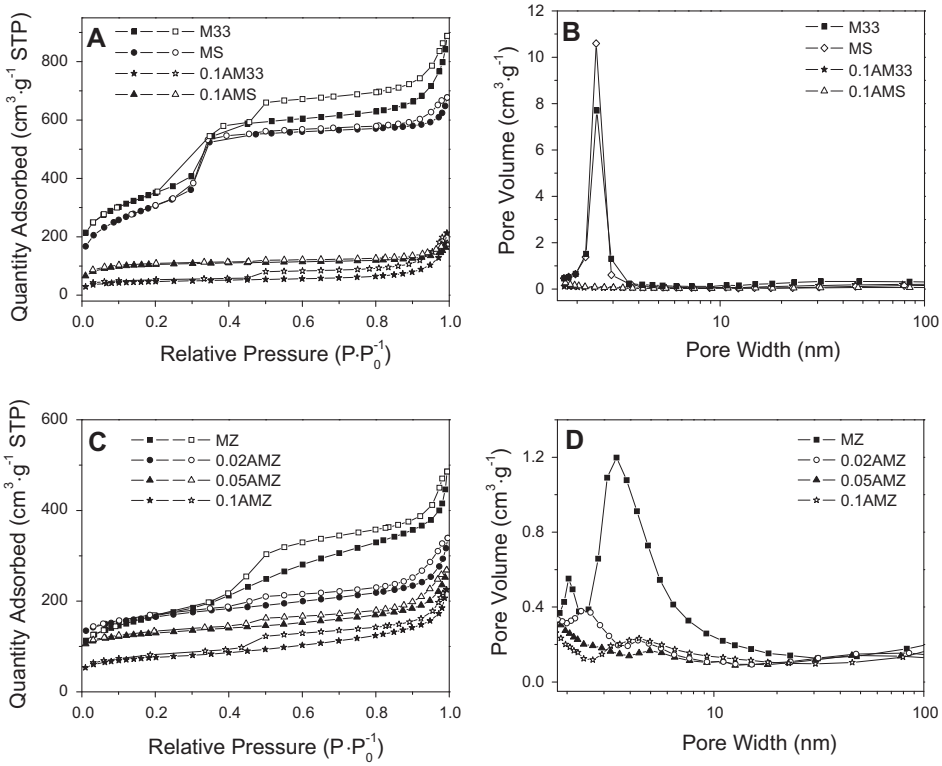

Fig. 2. Nitrogen adsorption–desorption isotherms (A and C) and pore size distributions (B and D) of MCM-41 series samples. The isotherms of M33, 0.02AMZ, and 0.05AMZ were offset vertically by 50, 70, and 50 $cm^3\ g^{-1}$, respectively.

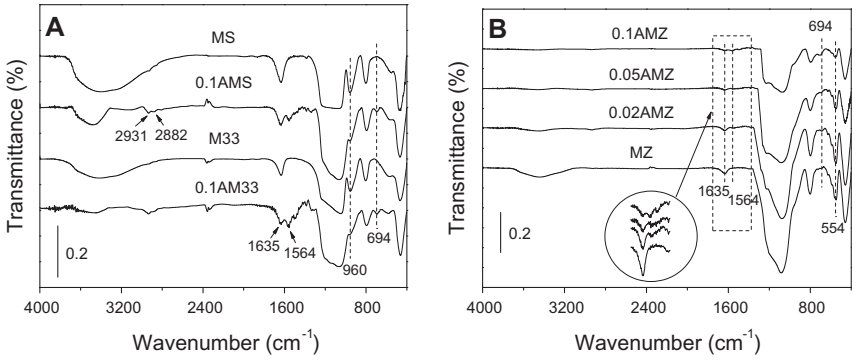

Fig. 3. FTIR spectra of MCM-41 series samples.

concentration of silanol groups (Fig. 3A). Two bands at 694 and 1564 cm^{-1}, attributed to N–H bending vibration and symmetric NH_2 bending vibration, respectively, were observed on the 0.1AMS and 0.1AM33 samples, confirming the presence of amino

groups [41]. The bands at 2931 and 2882 cm^{-1}, assigned to the stretching vibration of $-CH_2$ groups, were also observed on these samples. Nonetheless, the band of N–H bending vibration (1635 cm^{-1}) was overlapped while the asymmetric and symmetric stretching vibration of the $-NH_2$ groups could not be detected at 3300–3400 cm^{-1}, because of the existence of O–H bending vibrations of adsorbed water molecules [41]. The postmodified silicas had weak bands near 3440 and 960 cm^{-1}, because of their hydrophobic surfaces [42]. Fig. 3B depicts the IR spectra of MZ and *n*AMZ samples. A strong band at 554 cm^{-1} was observed on the spectrum of MZ, indicating the formation of a crystalline zeolitic structure [35]. Also, the Si–OH band of 960 cm^{-1} almost disappeared on MZ, confirming further the zeolitic structure of this composite. The bands at 694 and 1564 cm^{-1} emerged on *n*AMZ samples, and their intensities rose with more APTES modifier loaded (Table 1). However, fewer organic groups were anchored on 0.1AMZ than on 0.1AMS and 0.1AM33 (Table 1 and Fig. 3), because MZ had a lower silanol concentration than MS and M33. Besides, the *n*AMZ sample had a more hydrophobic surface than MZ so that it adsorbed fewer water molecules (Fig. 3B).

3.2. Actual performance of the multifunctional biochemical vessel

Fig. 4 illustrates the release curves of NO from aminopropyl-functionalized samples in the mimic gastric juice at 310 K, in which the released amount of NO increased as the amount of aminopropyl groups rose. According to the detected amount of NO at 120 min in the test, the APTES-modified composites released several times more NO in the solution than their parents. In the mimic gastric juice without nitrosamines, the released amount of the 0.1AZ sample was three times more than that of HZSM-5 zeolite, while the *n*AMZ composites released 20 times more NO than MZ sample (Table 2). The highest value emerged on 0.1AM33 whose released amount was 59 times higher than that of M33, and the runner up was 0.1MS that released 34 times more NO in the solution than mesoporous silica MS. In the mimic gastric juice containing NPYR, the organic-modified mesoporous composites exhibited a higher release capability than their parents (Table 2 and Fig. 4A and B). The 0.1AMZ released 36 times more NO than MZ, 0.1AMS was 49 times higher than MS, and the largest promotion was still found on the 0.1AM33 sample that released 74 times more NO than M33 under the same conditions. Also, most of the APTES-modified samples released more NO at 120 min in the solution containing NPYR than that without NPYR (Table 2). A similar situation appeared in the solution containing NNN where all samples exhibited a higher release capability than that in mimic gastric juice itself. Subsequently, the promotion of organic modification on the release of NO was lowered, and the 0.1AM33 sample released 26 times more than M33 (Table 2 and Fig. 4). Different NO-release behavior of the sample in the solution with NPYR or NNN probably resulted from the different properties of NPYR and NNN such as polarity, alkalescence, and hydrophilic/hydrophobic properties, but further investigation is required to explore the mechanism.

Modification of molecular sieves with the aminopropyl group indeed enhanced their NO-delivery ability, and the released NO amount could be tuned in the range of 1.68–37.12 μmol g^{-1} through varying the NO-delivery silica supports and loading amounts of organic groups (Tables 1 and 2). To accurately assess the release ability of samples without the influence of surface area, we can calculate their released amount in unit area (nmol m^{-2} instead of μmol g^{-1}). For instance, the corresponding value of M33 and 0.1AM33 in the solution containing NPYR was 0.4 and 202 nmol m^{-2}, while that of MZ and 0.1AMZ was 1.0 and 87.3 nmol m^{-2}, respectively. Clearly the modification of molecular sieves with APTES is crucial for increasing their capability of releasing NO in mimic gastric juice, tailoring their surface state through grafting aminopropyl groups on their surface. Moreover, the release capability of APTES-modified samples was consistent with their N content (Tables 1 and 2). For example, the amounts of NO released from 0.02AMZ and 0.05AMZ samples were similar because of the similar N contents of the two samples (2.03 and

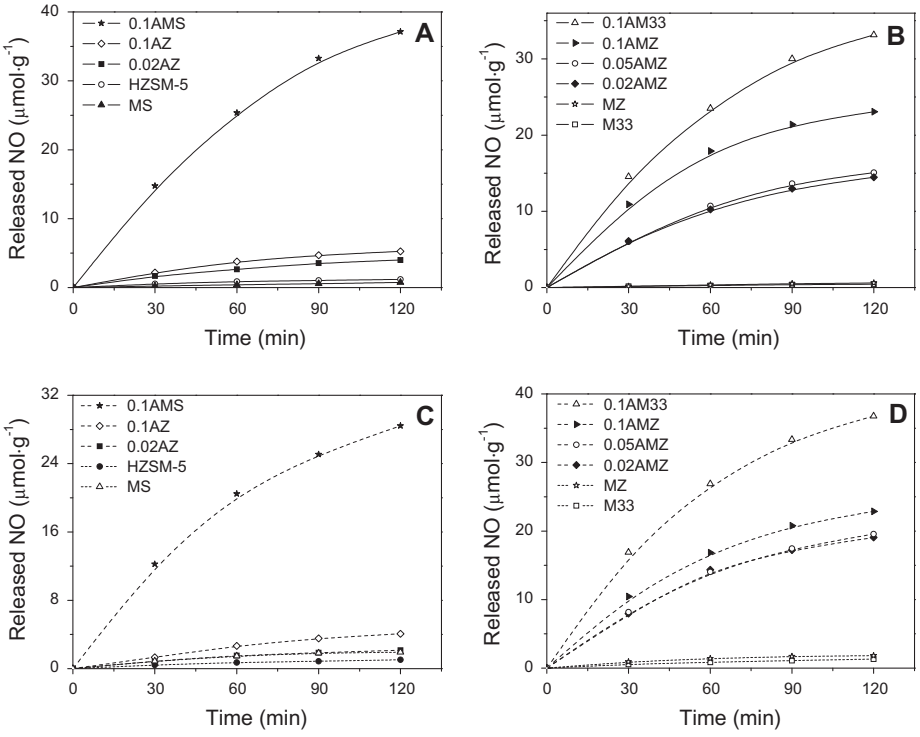

Fig. 4. Release curves of NO in mimic gastric juice containing (A and B) NPYR and (C and D) NNN on the samples preadsorbed with NO at 310 K.

Table 2
The results of NO desorbed in the mimic gastric juice without or with NPYR/NNN[a] on the samples preadsorbed with NO.

Sample	NO released in the solution without nitrosamine ($\mu mol\ g^{-1}$)			NO released in the solution with NPYR ($\mu mol\ g^{-1}$)			NO released in the solution with NNN ($\mu mol\ g^{-1}$)		
	30 min	Total	Increment (%)[b]	30 min	Total	Increment (%)[b]	30 min	Total	Increment (%)[b]
HZSM-5	0.50	1.00	–	0.55	1.20	–	0.44	1.04	–
0.02AZ	0.50	1.68	68	1.69	4.00	233	0.90	2.15	107
0.1AZ	1.43	3.99	299	2.19	5.25	338	1.33	4.09	293
MZ	0.37	0.67	–	0.17	0.61	–	0.91	1.82	–
0.02AMZ	5.56	14.15	2012	6.10	14.46	2270	7.95	19.07	948
0.05AMZ	7.89	14.74	2100	6.02	15.08	2372	8.17	19.55	974
0.1AMZ	8.76	19.99	2884	10.92	23.05	3679	10.44	22.87	1157
M33	0.22	0.44	–	0.16	0.44	–	0.57	1.32	–
0.1AM33	10.60	26.50	5923	14.55	33.14	7432	16.89	36.76	2685
MS	0.36	0.77	–	0.23	0.73	–	0.88	1.92	–
0.1MS	10.82	27.43	3462	14.75	37.12	4985	12.24	28.42	1380

[a] The acid-induced release of NO was carried out at 310 K, the pH value of solution was 1.2, and the total NO release time was fixed at 2 h.
[b] Increment percentage of the released NO amount on aminopropyl-modified sample in comparison with the corresponding parent material.

2.29 wt.% of N, Table 1). It should be pointed out that these organic-modified composites have many advantages in comparison with common zeolites such as NaA and NaY, because these zeolites released less NO in the acidic solution and/or their structures were easily destroyed [24].

Modification of molecular sieves with APTES had a complex influence on their adsorption of nitrosamines in mimic stomach juice because a lot of surface silanol groups were consumed in the process. Zeolite and mesoporous silica samples could trap nitrosamines in the solution even though they had preadsorbed NO. HZSM-5 zeolite adsorbed 0.71 mg g^{-1} of NPYR, more than mesoporous samples MZ, M33, and MS. The MZ sample captured more NPYR (0.58 mg g^{-1}) than MS and M33, because of the existence of a ZSM-5 zeolitic structure (Table 1) [35]. Nonetheless, *n*AZ samples adsorbed less NPYR than parent HZSM-5, and their adsorption capacity decreased as the amount of aminopropyl groups increased, which originates from the lowered surface area since the adsorption capability of unit surface area was increased indeed (Table 1). The 0.1AMS and 0.1AM33 samples failed to adsorb NPYR in the solution, because their silanol groups had been consumed during modification with APTES and the silanol group was the main adsorptive site of mesoporous silica toward nitrosamines [43]. A similar situation was also observed on *n*AMZ composites whose adsorption ability of NPYR was lower than MZ (Table 1). However, the amount of NPYR adsorbed by *n*AMZ samples slightly increased as their micropore surface area rose on a small scale, illustrating the important role played by the micropore in *n*AMZ samples.

To explore the influence of preadsorbed NO on the adsorption of nitrosamines, Fig. 5 reveals the release amount of NO and

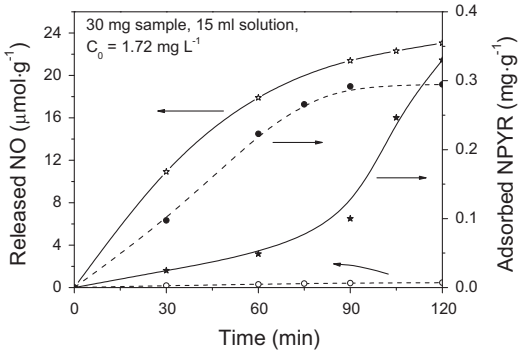

Fig. 5. Release of NO and adsorption of NPYR by 0.1AMZ sample preadsorbed with NO (solid line) and 0.1AMZ sample nonadsorbed NO (dashed line) vs. time in the mimic gastric juice at 310 K.

adsorption ability of NPYR by two samples of 0.1AMZ, preadsorbed NO or fresh, in the mimic gastric juice at 310 K. The preadsorbed NO sample had a burst release of NO in the beginning but gradually cooled down, meanwhile less NPYR was captured at first, followed by a sharp increase in adsorption (Scheme 1). Concretely, about 93% of NO was released at 90 min (Fig. 5), but about 0.1 mg g^{-1} of NPYR was trapped, equaling one-third of the total adsorbed by the sample (0.33 mg g^{-1}, Table 1). In contrast, the fresh sample trapped 0.1 mg g^{-1} of NPYR in 30 min and achieved its adsorption equilibrium within 90 min, although its capacity (0.30 mg g^{-1}, Fig. 5) was slightly smaller. Less NO was also detected in the solution, attributed to the degradation of nitrosamine on the sample. It seems that surface nitrous species on the mesoporous zeolite preadsorbed with NO delays the adsorption of nitrosamine, since the main adsorption occurred after the majority of release.

Another nitrosamine, NNN, could also be captured by zeolite and mesoporous silica in mimic gastric juice. MS and M33 mesoporous samples adsorbed more NNN than HZSM-5 zeolite because of their large pore size. NNN has a molecular size (0.54 × 0.80 nm, Scheme S1) larger than the pore diameter of HZSM-5, so it had to insert the N–NO group into the channel and this inserting model of adsorption was slow [40]. Modification of the aminopropyl group made the surface of *n*AZ samples more hydrophobic to weaken the competition adsorption of water, leading to more NNN adsorbed (Table 1) [32], because the hydrophobic nitrosamine was prone to be adsorbed on the hydrophobic sample. The wide channel of mesoporous silica and the interaction from the surface silanol group induced more NNN to be trapped in MS and M33 [40]. However, these mesoporous adsorbents became inferior after modification with APTES, because of the decreased surface area, pore volume, and silanol numbers. A complex phenomenon appeared on *n*AMZ composites that had a combined structure of mesoporous silica and zeolite. About 0.33 mg g^{-1} of NNN was adsorbed by MZ, equal to that by parent M33, thanks to the stronger electrostatic field and the existence of mesopores. The adsorption capability of 0.02AMZ declined clearly, similar to the phenomenon observed on MS and M33; however, more NNN were adsorbed on other *n*AMZ samples with more organic groups due to their enhanced surface hydrophobic properties. On the basis of the adsorption capability of unit surface area of composite (Table 1), it is evident that APTES modification really enables the composite to adsorb more hydrophobic NNN.

3.3. Explore the release mechanism of NO in acid solution

Fig. 6A shows the *in situ* FTIR spectra of NO adsorbed on MZ sample to investigate the surface nitrous species formed. The bands at

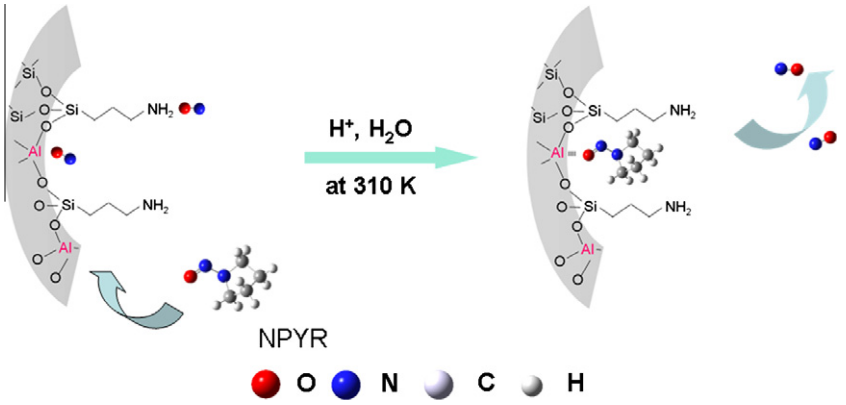

Scheme 1. NO release and nitrosamine capture by aminopropyl-functionalized silica matrix in gastric mimic juice.

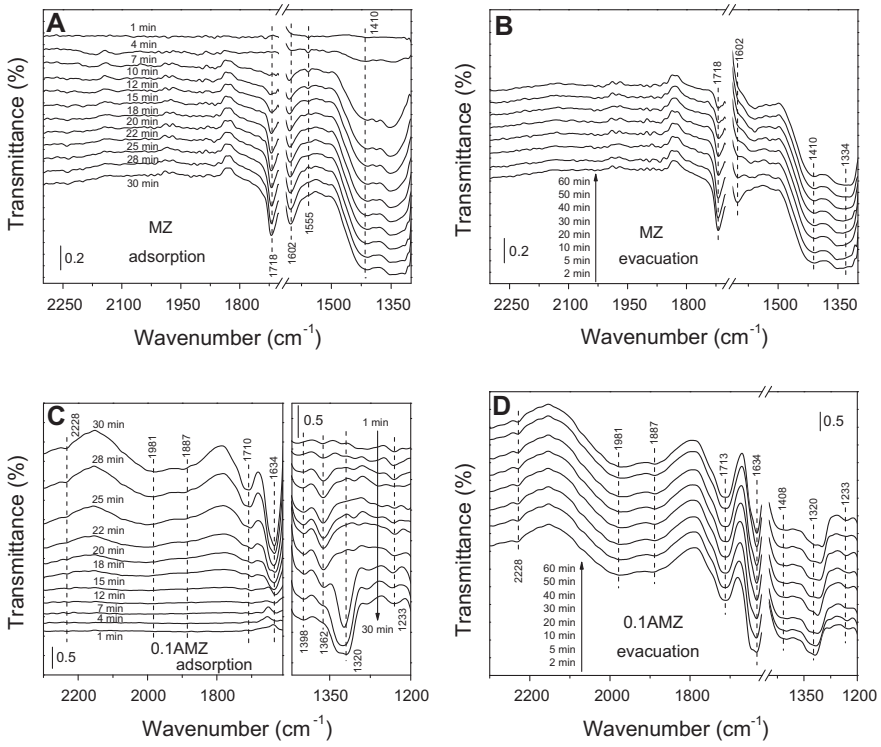

Fig. 6. *In situ* FTIR spectra of MZ and 0.1AMZ samples that adsorbed NO (1.98% in volume) (A and C) and evacuated (B and D) at 310 K.

1602, 1410, and 1354 cm^{-1} formed quickly on MZ in contact with NO, which were assigned to bidendate nitrates and υ_3 mode splitting of surface nitrate adsorbed on Na^+ sites [44,45]. Concomitantly, the band attributed to $(NO)_2$ dimeric species also appeared at 1718 cm^{-1} [46]; further exposure of MZ to NO strengthened those bands of nitrates and $(NO)_2$. The intensity of the 1555 cm^{-1} band, assigned to N_2O_3, was increased at first, but declined soon and finally disappeared (Fig. 6A). After the sample was purged with N_2 for 1 h, the intensity of Na^+–nitrate bands remained invariant, while those of bidendate nitrates and $(NO)_2$ decreased. Meanwhile, the band of N_2O_3 emerged once again, indicating the different stabilities of surface nitrous species on the sample (Fig. 6B). Judging from these results, it is clear that the main nitrous species on MZ were nitrates that were reduced to NO only at elevated temperatures but not decomposed in acidic solution.

Fig. 6C represents the *in situ* FTIR spectrum of the 0.1AMZ sample. Apart from the bands of $(NO)_2$, N_2O, and NO emerged at 1710, 2228, 1887, and 1981 cm^{-1}, bands of monodentate nitrate at 1634 cm^{-1} and bidentate nitrite around 1233 cm^{-1} were also observed [47]. Besides, the bands centered at 1320, 1362, and 1398 cm^{-1} were assigned to unidentate nitrates and the nitrates associated with Na^+, respectively; in particular, the 1320 cm^{-1} band might be transformed from Na^+–nitrate species [44]. When the sample of 0.1AMZ was exposed to NO, a band appeared at 1362 cm^{-1}, and its intensity increased up to 22 min, but declined quickly and finally disappeared. At the same time, a 1320 cm^{-1} band of unidentate nitrates formed and grew up (Fig. 6C). Their intensity did not change even when the sample was purged at 310 K for 1 h, implying the high stability of surface nitrous species (Fig. 6D). It appears that the main surface nitrous species on the 0.1AMZ sample were N_2O, NO, $(NO)_2$, and nitrites. They were easy to be induced, releasing large amounts of NO in acid solution, which is the main reason why the 0.1AMZ sample released more NO than MZ in mimic gastric juice.

4. Discussion

It is safer to release NO by zeolites through the digestive system than through the circulatory system because this strategy avoids the formation of blood clots. Also, this release is acid-triggered instead of water-triggered so that moisture-saturated zeolites can be used as the vessel, and they no longer require activation prior to the adsorption of NO along with the rigorous anhydrous storage [24]. Besides, the zeolite vessel is able to trap nitrosamines in gastric juice, preventing the carcinogen from metabolic activation [26]. These advantages make the releasing of NO through the digestive system attractive and competitive. Two factors are vital for zeolite to play both roles of releaser and trapper in the "adsorption-release-adsorption" process. The first is the suitably high Si/Al ratio of zeolite, which not only suppresses the competitive adsorption of water but also has adequate electrostatic affinity toward nitrosamines [25]. A high Al content of zeolite usually couples with a large number of cations in the framework such as NaA, which is beneficial for adsorbing NO [5,38], but is improper for the acid-triggered release of NO because of the acid-induced structural decomposition in gastric juice [25]. On the contrary, a low Al content of zeolite goes against the adsorption of NO since cations such as Na^+ ions in the zeolites are favorable for NO storage under the experimental conditions [44]. Also, lack of enough cation in the zeolite fails to establish a powerful electrostatic interaction in the channel; therefore, the zeolite will have a weak activity for adsorbing nitrosamines [29,33]. Based on our previous investigation [25,26], the HZSM-5 zeolite with a Si/Al ratio of 20 is chosen, accompanied with mesoporous ZSM-5 zeolite and Al-containing and siliceous mesoporous MCM-41, in order to examine the influence of mesopores, zeolitic structure, and Al components in the composites on the release of NO in mimic gastric juice. As demonstrated in Table 2, HZSM-5 zeolite released more NO than MZ composite because of the promotion of cation in the zeolite on NO storage [5,38]. The MZ sample is the zeolitic material transformed from the as-synthesized mesoporous silica; hence it has less cation than HZSM-5 zeolite [35], resulting in a release performance inferior to zeolite HZSM-5. A different situation was observed on mesoporus silica in which the MS sample released a larger amount of NO than M33, since MS has more silanol groups than M33 (Fig. 3A), and silanol groups play a crucial role in the adsorption of mesoporous silica [43]. On the other hand, the property–function relationship of these composites is obvious in the adsorption of nitrosamines in mimic gastric juice: zeolitic structure and the Al component of mesoporous silica are favorable for the adsorption of NPYR (Table 1), while the mesopores of adsorbents promote the adsorption of bulky nitrosamines NNN [26,40,43].

The second factor is the special organic modification of zeolite and mesoporous silica, which ensures that these vessels exhibit a dramatically enhanced ability of releasing NO. Modification of APTES is essential for three reasons. First, APTES modification avoids the drawback of easy formation of nitrosamines and leaching of amino groups that were reported in diamine-functionalized silica support [30,31]. The sample of 0.1AMZ preadsorbed with NO was added into distilled water but no NO was detected in the suspension. This fact excluded the formation of *N*-diazeniumdiolate on 0.1AMZ. Otherwise, the nitrosamine precursor was unstable and easily reduced to NO in the presence of water. Moreover, no nitrosamine was detected when the aminopropyl-modified sample preadsorbed with NO was added into acidic solution, either, indicating the feasibility and safety of the organic modification. Second, APTES induces the adsorbed NO to form nitrites and $(NO)_2$ on the surface of adsorbent, inducing a larger amount of NO to be released in acidic solution (Fig. 6 and Table 2) because nitrites provide another active storage of NO [24]. A large amount of nitrite was detected when the sample preadsorbed with NO was added into distilled water, so that nitrite would be desorbed at first when the porous materials encountered water. Subsequently, the desorbed nitrite was reduced to NO in the presence of proton, because NO formation resulting from the decomposition of free nitrous acid was strongly pH dependent [24]. Third, APTES is thermal stable below 500 K [48], which ensures its safe use in ambient temperature. Different from those diamine-modified silica samples, amino groups of the APTES-modified molecular sieves are stable and no leaching of amino groups occurs in mimic gastric juice. Also, the hydrophobic property of APTES is beneficial for the modified composite to suppress the competitive adsorption of water in the acidic solution [32].

The actual function of APTES modification depended on the structure of the aluminosilicate molecular sieve. HZSM-5 zeolite specializes in adsorption of volatile nitrosamines and releasing NO thanks to its microporous channel and cations. However, APTES was difficult to be grafted in HZSM-5 due to the lack of a silanol group in the zeolite, and the bulky modifier could not enter the narrow channel of HZSM-5 so that the loading efficiency of APTES was low (Table 1) and the modifiers mainly located on the external surface or near the pore mouths of zeolites. As the result, only a minor effect was produced on the NO-delivery performance of 0.1AZ that only released two times more NO than the parent zeolite HZSM-5.

Siliceous MCM-41 has plenty of surface silanol groups and wide channels; hence it is able to trap more NNN and graft more aminopropyl groups than HZSM-5 zeolite. Therefore 0.1AMS samples released the NO 10 times higher than 0.1AZ (Table 2). However, APTES modification consumed a lot of surface silanol groups (Fig. 3A); the grafted aminopropyl groups also narrowed the channel. Such narrowed channels were easily characterized by the nitrogen adsorption at 77 K, similar to that reported on the amine-coated or organic-modified MCM-41 [32,49], resulting in a dramatically lowered surface area of 0.1AMS (from 1119 to 366 $m^2\ g^{-1}$). Incorporation of aluminum in the sample of M33 created some large pores in the composite (Fig. 2A), which led to 25% more aminopropyl groups to be grafted in M33 than in MS and caused a high increment in NO release (Table 2). It should point out that APTES modification weakened the adsorption ability of mesoporous silica toward nitrosamines in mimic gastric juice, because a lot of silanol groups were consumed and these silanol groups were the main adsorption site of mesoporous silica [43]. Thereby, either 0.1AM33 or 0.1AMS sample failed to trap NPYR and adsorbed only a small quantity of NNN in mimic gastric juice (Table 1). Incorporation of Al in the framework of M33 enabled the composite to adsorb more NPYR than MS in the solution (Table 1), but 0.1AM33 was inactive for capturing the volatile nitrosamine, which probably was due to the coverage of adsorption sites by adjacent aminopropyl groups but further study was required to study the mechanism.

Mesoporous zeolite MZ consisted of both microporous and unordered mesoporous structures [35]; hereby it had a high capacity in releasing NO and capturing nitrosamines (Tables 1 and 2). Rather, the hierarchical structure of MZ enabled the composite to keep the microporous surface area after the modification with APTES (Table 1), since the organic modifier preferred to occupy the large pores as aforementioned. As the result, a lot of aminopropyl groups were grafted in the unordered mesopores; for example, 0.1AMZ had a N content (4.08%, Table 1) similar to 0.1AMS (4.30%) but its microporous surface area was stayed at 117 $m^2\ g^{-1}$ (Table 1), close to that of MZ (121 $m^2\ g^{-1}$). Accordingly, the 0.1AMZ sample could release the NO 10 times more than its parent MZ, and at the same time it was able to adsorb 38–50% of the nitrosamines in mimic gastric juice (Fig. 4 and Table 1). These results imply the

potential application of mesoporous zeolite to release NO and adsorb nitrosamines in the digestive system.

Fabrication of an optimal vessel is crucial for performing the strategy of "releasing NO–capturing nitrosamines" through the digestive system, for which the ideal multifunctional biomaterials should have plenty of silanol groups for grafting aminopropyl groups to significantly enhance the capability of NO release; also it must possess a zeolitic structure with cations to promote adsorption of nitrosamines. However, zeolites are propitious for adsorbing nitrosamines but their capability of releasing NO needs to be enhanced. Yet, the narrow channel of HZSM-5 is a drawback for APTES modification so that the modifier only reacts with the terminal silanol groups located on the external surface of zeolite to form the limited aminopropyl groups. On the contrary, mesoporous silica has wide channels and plenty of silanol groups for the APTES modifier, but it is weak in adsorbing volatile nitrosamines such as NPYR. Thus, it will be a challenge to combine the advantages of zeolite and mesoporous silica to form multifunctional biomaterial. Incorporating Al in the framework of MCM-41 slightly promotes the grafting of APTES but weakens the adsorption of nitrosamines as aforementioned. Thereby, mesoporous zeolite becomes the competitive candidate because it contains a zeolitic structure along with nonordered mesopores covered by silanol groups. Consequently, APTES modification is controllably performed on the mesoporous area while the zeolitic structural area is protected. The special phenomenon reflects the advantage of hierarchical structure on the organic modification, affording a valuable clue for the preparation of multifunctional biomaterials to elevate the efficiency of zeolites in other applications such as drug delivery.

5. Conclusion

(1) The controlled release of NO and the trapping of nitrosamines simultaneously was realized in mimic gastric juice by zeolite, mesoporous zeolite, and mesoporous silica, elevating the efficiency of these functional materials in health care.
(2) APTES modification enables zeolite and mesoporous silica to release several times more NO in mimic gastric juice. NO adsorbed on the modified composites is able to form surface species such as nitrites and $(NO)_2$, leading to more NO to be released in acidic solution. The vessel preadsorbed NO will give out NO at first, and then capture NPYR, releasing NO in a wide range of 1.68–37.12 $\mu mol\ g^{-1}$ and trap the nitrosamines up to 82.6% in the solution.
(3) Mesoporous ZSM-5 zeolite possesses both structural advantages of zeolite and mesoporous material; therefore, controllable APTES modification can be realized on this hierarchical material, in which the structure of zeolite is maintained while a lot of aminopropyl groups are grafted. As the result, the resulting composite exhibits a high capability of releasing NO and adsorbing nitrosamines in mimic gastric juice.

This study is our preliminary approach for developing zeolite functional materials for releasing nitric oxide through the digestive system. Further investigations are required to clearly identify detailed characteristics of the process.

Acknowledgments

Financial support from NSF of China (20773061 and 20873059), Grant 2008AA06Z327 from the 863 Program, and Analysis Center of Nanjing University is gratefully acknowledged.

Appendix A. Supplementary material

Supplementary data associated with this article can be found, in the online version, at doi:10.1016/j.jcis.2011.01.019.

References

[1] X.X. He, J.Y. Chen, K.M. Wang, D.L. Qin, W.H. Tan, Talanta 72 (2007) 1519.
[2] E. Ruiz-Hitzky, M. Darder, P. Aranda, K. Ariga, Adv. Mater. 22 (2010) 323.
[3] D. Chitkara, A. Shikanov, N. Kumar, A.J. Domb, Macromol. Biosci. 6 (2006) 977.
[4] J.T. Zhang, T.F. Keller, R. Bhat, B. Garipcan, K.D. Jandt, Acta Biomater. 6 (2010) 3890.
[5] P.S. Wheatley, A.R. Butler, M.S. Crane, S. Fox, B. Xiao, A.G. Rossi, I.L. Megson, R.E. Morris, J. Am. Chem. Soc. 128 (2006) 502.
[6] Q.M. Ji, M. Miyahara, J.P. Hill, S. Acharya, A. Vinu, S.B. Yoon, J.S. Yu, K. Sakamoto, K. Ariga, J. Am. Chem. Soc. 130 (2008) 2376.
[7] B.E. Mann, R. Motterlini, Chem. Commun. (2007) 4197.
[8] H.P. Zhang, G.M. Annich, J. Miskulin, K. Osterholzer, S.I. Merz, R.H. Bartlett, M.E. Meyerhoff, Biomaterials 23 (2002) 1485.
[9] C. Napoli, L.J. Ignarro, Annu. Rev. Pharmacol. Toxicol. 43 (2003) 97.
[10] L.A. Holowatz, W.L. Kenney, Am. J. Physiol.: Heart C 293 (2007) H1090.
[11] S. Shastry, N.M. Dietz, J.R. Halliwill, A.S. Reed, M.J. Joyner, J. Appl. Physiol. 85 (1998) 830.
[12] X.G. Sun, K.M. Kaltenbronn, T.H. Steinberg, K.J. Blumer, Mol. Pharmacol. 67 (2005) 631.
[13] M. Obst, J. Tank, R. Plehm, K.J. Blumer, A. Diedrich, J. Jorden, F.C. Luft, V. Gross, Am. J. Physiol.: Regul. Integr. Comp. Physiol. 290 (2006) R1012.
[14] P.G. Parzuchowski, M.C. Frost, M.E. Meyerhoff, J. Am. Chem. Soc. 124 (2002) 12182.
[15] H.P. Zhang, G.M. Annich, J. Miskulin, K. Stankiewicz, K. Osterholzer, S.I. Merz, R.H. Bartlett, M.E. Meyerhoff, J. Am. Chem. Soc. 125 (2003) 5015.
[16] J.T. Mitchell-Koch, T.M. Reed, A.S. Borovik, Angew. Chem., Int. Ed. 43 (2004) 2806.
[17] A.B. Seabra, N. Durán, J. Mater. Chem. 20 (2010) 1624.
[18] C. Buzea, I.I. Pacheco, K. Robbie, Biointerphases 2 (2007) MR17.
[19] A.C. McKinlay, B. Xiao, D.S. Wragg, P.S. Wheatley, I.L. Megson, R.E. Morris, J. Am. Chem. Soc. 130 (2008) 10440.
[20] H.A. Liu, K.J. Balkus Jr., Chem. Mater. 21 (2009) 5032.
[21] M. Mowbray, X.J. Tan, P.S. Wheatley, R.E. Morris, R.B. Weller, J. Invest. Dermatol. 128 (2008) 352.
[22] C.H.A. Cho, K.K. Wu, S. Wu, T.M. Wong, W.H.L. So, E.S.L. Liu, K.M. Chu, V.Y. Shin, Y.N. Ye, B.C.Y. Wong, Eur. J. Pharmacol. 460 (2003) 177.
[23] Y. Li, W.P. Wang, H.Y. Wang, C.H. Cho, Eur. J. Pharmacol. 399 (2000) 205.
[24] F. Wei, J.Y. Yang, Q. Hou, J.H. Zhu, New J. Chem. 34 (2010) 2897.
[25] C.F. Zhou, J.H. Zhu, Chemosphere 58 (2005) 109.
[26] X. Dong, C.F. Zhou, M.B. Yue, C.Z. Zhang, W. Huang, J.H. Zhu, Mater. Lett. 61 (2007) 3154.
[27] O. Schäf, V. Wernert, H. Ghobarkar, P. Knauth, J. Electroceram. 16 (2006) 93.
[28] Y.H. Jeong, S.S. Wang, Biotechnol. Technol. 6 (1992) 341.
[29] C.F. Zhou, Z.Y. Yun, Y. Xu, Y.M. Wang, J. Chen, J.H. Zhu, New. J. Chem. 28 (2004) 807.
[30] S.M. Marxer, A.R. Rothrock, B.J. Nablo, M.E. Robbin, M.H. Schoenfisch, Chem. Mater. 15 (2003) 4193.
[31] E. Besson, J. Amalric, A. Mehdi, P.H. Mutin, J. Mater. Chem. 19 (2009) 5723.
[32] F. Wei, J.Y. Yang, L. Gao, F.N. Gu, J.H. Zhu, J. Hazard. Mater. 172 (2009) 1482.
[33] Y. Xu, J.H. Zhu, L.L. Ma, A. Ji, Y.L. Wei, X.Y. Shang, Microporous Mesoporous Mater. 60 (2003) 125.
[34] P. Van Der Voort, P.I. Ravikovitch, K.P.D. Jong, M. Benjelloun, E.V. Bavel, A.H. Janssen, A.V. Neimark, B.M. Weckhuysen, E.F. Vansant, J. Phys. Chem. B 106 (2002) 5873.
[35] M.B. Yue, L.B. Sun, T.T. Zhuang, X. Dong, Y. Chun, J.H. Zhu, J. Mater. Chem. 18 (2008) 2044.
[36] L. Gao, Y. Wang, J.Q. Wang, L. Huang, L.Y. Shi, X.X. Fan, Z.G. Zou, T. Yu, M. Zhu, Z.S. Li, Inorg. Chem. 45 (2006) 6844.
[37] Z.Y. Wu, Y.M. Wang, W.W. Huang, J. Yang, H.J. Wang, J.H. Xu, Y.L. Wei, J.H. Zhu, Chem. Mater. 19 (2007) 1613.
[38] J. Yang, T.T. Zhuang, F. Wei, Y. Zhou, Y. Cao, Z.Y. Wu, J.H. Zhu, C. Liu, J. Hazard. Mater. 162 (2009) 866.
[39] W. Hammond, E. Prouzet, S.D. Mahanti, T.J. Pinnavaia, Microporous Mesoporous Mater. 27 (1999) 19.
[40] F. Wei, F.N. Gu, Y. Zhou, L. Gao, J. Yang, J.H. Zhu, Solid State Sci. 11 (2009) 402.
[41] B.F. Shi, Y.S. Wang, Y.L. Guo, Y.Q. Wang, Y. Wang, Y. Guo, Z.G. Zhang, X.H. Liu, G.Z. Lu, Catal. Today 148 (2009) 184.
[42] D.D. Asouhidou, K.S. Triantafyllidis, N.K. Lazaridis, K.A. Matis, Colloids Surf., A 346 (2009) 83.
[43] C.F. Zhou, Y.M. Wang, Y. Cao, T.T. Zhuang, W. Huang, Y. Chun, J.H. Zhu, J. Mater. Chem. 16 (2006) 1520.
[44] Q. Yu, X.P. Wang, N. Xing, H.L. Yang, S.X. Zhang, J. Catal. 245 (2007) 124.
[45] M. Mihaylov, K. Hadjiivanov, D. Panayotov, Appl. Catal. B: Environ. 51 (2004) 33.

[46] M. Mihaylov, E. Ivanova, N. Drenchev, K. Hadjiivanov, J. Phys. Chem. C 114 (2010) 1004.
[47] P.T. Fanson, M.W. Stradt, J. Lauterbach, W.N. Delgass, Appl. Catal. B: Environ. 38 (2002) 331.
[48] A.S. Maria Chong, X.S. Zhao, J. Phys. Chem. B 107 (2003) 12650.
[49] M.B. Yue, L.B. Sun, Y. Cao, Y. Wang, Z.J. Wang, J.H. Zhu, Chem. Eur. J. 14 (2008) 3442.